Wide Speed Range Permanent Magnet Synchronous Generator Design for a DC Power System

Dongmin Miao[1,2], *Yves Mollet*[1], *Johan Gyselinck*[1], *and Jianxin Shen*[2]*

(1. Department of Bio, Electro And Mechanical Systems, Université Libre de Bruxelles, Brussels, 1050, Belgium;
2. Department of Electrical Engineering, Zhejiang University, Hangzhou, 310027, China)

Abstract: A wide speed range permanent magnet synchronous generator (PMSG) system is studied in this paper, including the PMSG design and comparative study on control strategies with a pulse width modulation (PWM) rectifier, the purpose of which is to regulate the DC-link voltage. It is of great importance to study the foregoing DC power system based on the PMSG and PWM rectifier, where vector control (VC) can be implemented and the corresponding field-weakening strategy can be realized by injecting a field-weakening current component without any auxiliary devices. Large machine inductance is desired in order to limit the short-circuit current and the loaded voltage drop. Different control strategies including VC, direct torque control (DTC) and direct voltage control (DVC) are studied and compared with both simulations and experiments.

Keywords: Wide speed range permanent magnet synchronous generator, PWM rectifier, vector control, field-weakening control, direct torque control, direct voltage control.

1 Introduction

DC power systems are rather common, which usually consist of one or more power sources[1-7], e.g., wind turbine in a stand-alone power generation system[2-3], aircraft generator in the more electric aircraft system[4-5], vehicle generators[7]. Many research groups have looked into this interesting issue recently. By way of example, Prof. M. F. Rahman studied the terminal voltage control in an isolated wind powered three-phase induction generator (IG), which is driven by a variable speed wind turbine and is excited by a PWM rectifier[8]. Prof. O. A. Mohammed analyzed the performance and the DC-bus voltage control of a wind-powered self-excited induction generator (SEIG) and a three-phase vector-controlled PWM converter[9]. He has also studied the DC-bus voltage control for parallel-integrated wind-based PMSG[10-11], e.g., in a sustainable energy conversion system[12].

Compared to the IGs and other candidates, permanent magnet synchronous generators (PMSGs) are often preferred thanks to their advantages such as high power density, high efficiency and flexible machine structures[5, 7, 10-11, 13].

Nowadays, the concept of more electric aircraft (MEA) is becoming more and more attractive for the aeronautical industry, and this may be a very interesting and promising application for DC power systems. MEA replaces much hydraulic, mechanical and pneumatic equipment for propulsion, control and auxiliary systems with electric equipment, aiming at optimizing the global energy and improving the efficiency, reliability and maintainability of the aircraft[14-15]. Therefore, all electrical subsystems (electrical sources and loads of the aircraft) can be connected with a power distribution bus to form an electrical power distribution system (EPDS). Compared with conventional power distribution structures, the DC EPDS presents significant weight reductions, reduced maintenance requirements and costs, increased aircraft reliability, and also increased passenger comfort[15]. DC power systems have advantages regarding the ease of paralleling DC electrical bus bars and integration with loads. Some DC power system specifications have been incorporated in the American aircraft standard SAE AS 1831 and the American military standard (AMS) MIL-STD-704E[16]. The 270V DC EPDS is worth great attention, and the stability of the DC-link voltage plays an important role in the system performance[17], which is, generally speaking, the most reliable configuration for sustaining operation even under severe supply transients, while large DC link capacitors would aid in maintaining the system voltage during transients[18]. Furthermore, AC systems require larger cables than the DC systems because of the reactive power flow, and at high frequencies the problem of skin effect occurs. Therefore, the generation and distribution voltage in the advanced aircrafts is mainly 270V DC, together with a 28V DC distribution for low power loads[19-21], where the DC bus is usually supplied by a wide-speed-range engine.

Power electronics is a key technology in the MEA. In the Boeing 787, the 270V DC system is supplied by four auto-transformer-rectifier units which convert the 235V AC power to the 270V DC power, supporting a handful of large-rated adjustable speed motors (including ram air fan motors, cabin pressurization compressor motors, and large hydraulic pump motors, etc.)[17]. However, PWM rectifiers (also called active rectifiers) can be connected to a variable PMSG and output the required DC voltage to the DC bus directly, which are superior in controllability compared to the alternative topologies (e.g., diodes

* Corresponding Author, E-mail: j_x_shen@zju.edu.cn.
Supported by the National Science Foundation of China (NSFC 51377140) and China Scholarship Council (CSC).

with DC/DC converters, thyristors, etc.), and can be chosen as the AC/DC converter between the PMSG and the DC-link.

However, the PMSG has a constant flux linkage excited by the magnets. The needed flux-weakening for high-speed operation is therefore not always easy due to the risk of demagnetizing the magnets, especially if this aspect is not taken into account during the machine design. The traditional vector control (VC) regulates these two components by controlling their corresponding current components[22]. The VC can have a fixed switching frequency, however, has complex coordinate transformation calculation and is parameter-dependent.

Another category of control strategy is the direct torque control (DTC), which regulates the flux linkage vector and further the torque of the PMSG directly, with the estimation of the stator flux linkage and the machine torque[13]. Discrete space voltage vectors can be chosen or SVPWM technology can be applied according to the status of the magnetic flux and the torque. The computational cost of the DTC is relatively high, mainly due to the estimation of the stator flux linkage. Moreover, the switching frequency of DTC is not fixed, but depends on the hysteresis widths of the torque and flux linkage hysteresis controllers. Nevertheless, the DTC is parameter-independent, except for the stator resistance.

The output electromagnetic power can be regulated directly by the voltage components, thus, direct voltage control (DVC) is proposed by controlling the amplitude of the stator voltage vector and the power angle between the stator voltage vector and the back EMF vector[23]. Another form of direct voltage field oriented control (DVFOC) is studied in[23], which is a derivative of the traditional VC by skipping the current loops when the current dynamics is fast enough, compared to the voltage dynamics. In this paper, VC, DTC and the proposed DVC are studied and compared through theoretical analysis, simulation and experiments.

2 Power conversion topology selection

Power electronics plays an important role in the integration of future renewable energy systems and design of generator systems. The AC power generated by the PMSG can be converted to a DC power via an AC/DC converter. The main categories of AC/DC converter usually include the diode rectifier, the thyristor rectifier, and the PWM rectifier.

The studied system usually works over a wide speed range due to the highly variable and unpredictable speed of the prime mover. The simplest structure of three-phase diode rectifier is used to convert AC voltage to DC voltage in an uncontrolled manner. The PMSG with a diode rectifier will generate a DC output voltage which is foremost determined by the rotor speed. When the speed is changing over a wide range, the DC output voltage after the diode rectifier also changes significantly. This type of rectifier has the advantage of being simple, robust, and low cost. However, it allows only unidirectional power flow, while has a non-unitary power factor and draws a highly distorted current from the PMSG, and a large volume DC-link capacitor is required.

In order to further regulate the output DC voltage, i.e., increase or decrease it, a DC/DC converter has to be connected between the diode rectifier and the DC-link capacitor. The main drawback of this solution, besides the diode rectifier presence, is the stress on the power switch.

2.1 Boost converter

A boost converter (see Fig.1) is a step-up DC/DC converter, with an output voltage U_o greater than the input voltage U_i. The switch S_a is typically a MOSFET or an IGBT, and the duty cycle α of the switch is defined as in (1). Here, t_{on} is the turn-on time duration and T is the time for one period. Inevitably, α is always greater than or equal to 0 and less than or equal to 1.

$$\alpha = \frac{t_{on}}{T} \tag{1}$$

Supposing the DC current in the inductor L_a is continuous, the relationship between the input and the output voltages is calculated as in (2). Here, U_i is the input voltage of the DC/DC converter, and is the output voltage generated from the diode rectifier after the PMSG as well; U_o is the output voltage of the DC/DC converter.

$$\frac{U_o}{U_i} = \frac{T}{T - t_{on}} = \frac{1}{1-\alpha} \tag{2}$$

If a boost converter is used in the proposed wide speed range PMSG system to convert the input voltage U_i to a greater (or equal) output voltage U_o, it means when the machine speed is approaching the lower limit, the input voltage U_i is much lower than U_o, and the duty cycle α of the booster needs to be very close to 1; when the speed is high enough and approaching the upper limit, the input voltage U_i is just slightly less than U_o^*, and the duty cycle α should be very close to 0. Both cases lead to very bad current waveforms, even when the inductor L_a is very large. Moreover, if the PMSG system operates in the constant power mode and the machine speed varies over a wide range, for example, by 10 times, then the current in the switches at the lowest speed is 10 times that at the highest speed. This will cause a very severe current stress on the switches at low speeds.

2.2 Buck converter

A buck converter (see Fig.2) is a step-down DC/DC

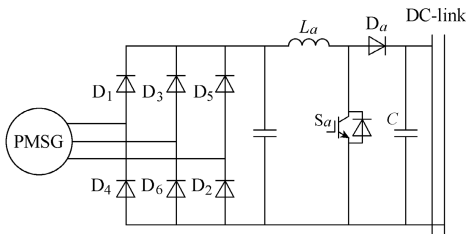

Fig.1 PMSG system with diodes and boost converter

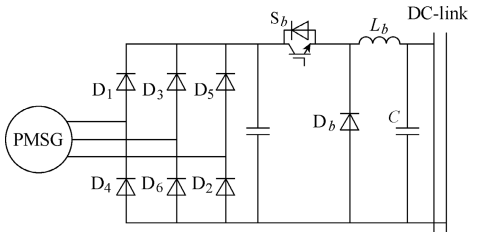

Fig.2 PMSG system with diodes and buck converter

converter, with an output voltage U_o less than or equal to the input voltage U_i. The switch is usually a MOSFET or an IGBT. To be the same as the case of a boost converter, when the DC current is continuous, the relationship between the input and the output voltage is calculated as in (3).

$$\frac{U_o}{U_i}=\frac{t_{on}}{T}=\alpha \tag{3}$$

If a buck converter is used in the proposed wide speed range PMSG system, to convert the input voltage U_i to a lower output voltage U_o, it means when the machine speed approaches the lower limit, the input voltage U_i should be slightly greater than U_o, and the duty cycle α of the switch needs to be very close to 1; when the speed approaches the upper limit, the input voltage U_i is then much greater than U_o, and the duty cycle α should be very close to 0. Both cases lead to very bad current waveforms. One more problem is that the voltage on the power switches at the highest machine speed is very high. For example, if the required U_o is 270V, and the machine speed varies by 10 times, then the voltage in the PMSG and on the switches would be up to 270V. This would cause very high stress on the switches and on the machine insulation.

2.3 Boost/buck converter

A boost/buck converter (see Fig.3) is a type of DC/DC converter with an output voltage U_o that can be either greater than or less than the input voltage U_i, and the output is of the opposite polarity of the input. To be the same with the boost converter or the buck converter, when the DC current is continuous, the relationship between the input and the output voltage is calculated as in (4). When α is 0.5, the output voltage U_o is equal to the input voltage U_i. When α is greater than 0.5, U_o is greater than U_i, and the converter is acting like a boost converter. When α is less than 0.5, U_o is less than U_i, and the converter is working as a buck converter.

$$\frac{U_o}{U_i}=\frac{t_{on}}{t_{off}}=-\frac{\alpha}{1-\alpha} \tag{4}$$

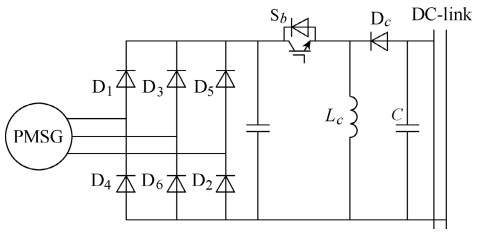

Fig.3 PMSG system with diodes and boost/buck converter

Compared with the boost converter or the buck converter, this converter has less severe current or voltage stress on the switches at the ultimate speeds, but the phase angle of the PMSG current is not strictly controlled, hence, the PMSG usually exhibits a low power factor.

2.4 Thyristor rectifier

Compared with other devices such as IGBT and MOSFET, the thyristor can bear the highest voltage and current, and has furthermore low price and high reliability. Although the switching frequency is low, it has prospects in high-power, low-frequency electronics devices. The line frequency phase-controlled converter topology is shown in Fig.4. The main disadvantages of this topology are the large current harmonics injected into the PMSG, and the poor power factor. The average DC output voltage is always lower than the amplitude of the input AC voltage; therefore, the performance of the PMSG system with thyristor rectifier is similar to that with diodes and buck converter. The amplitude of the imposed voltage on the thyristor is always the amplitude of the PMSG line-line voltage amplitude (U_{ab}), and the average DC output voltage is calculated as in (5) when the DC current is continuous.

$$U_d=\frac{U_{ab}}{\pi/3}\cos\theta \tag{5}$$

where θ is the firing angle of the thyristor.

2.5 PWM rectifier

In recent years, development in the PWM-controlled AC/DC rectifier made it a rather popular topology for various applications. This fully controlled topology, shown in Fig.5, has the advantages of using a low-cost three-phase module with a bi-directional energy flow capability as well as high quality DC output.

Given the condition that the PMSG is working over a wide speed range from n_{min} to n_{max}, e.g., 1:10, there would be a severe voltage stress on the winding insulation and the switches. When selecting the power

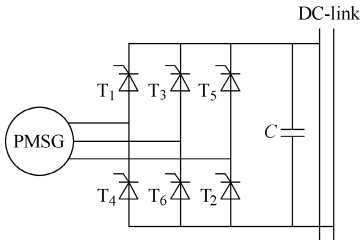

Fig.4 PMSG system with thyristor rectifier

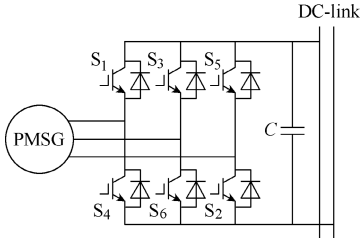

Fig.5 PMSG system with PWM rectifier

rating of the switches or power devices in each power conversion topology, the maximum open-circuit voltage and the short-circuit armature current of the PMSG should be taken into consideration if the adopted power conversion topology cannot regulate the output voltage on the machine-side. However, the output voltage of the PMSG can be fully controlled when using a PWM rectifier. Considering the synthesized factors of the system flexibility, reliability and controllability, the PWM rectifier is hereby selected as the most workable power converter between the PMSG and the DC-link.

3 PMSG machine design

For a constant-speed PMSG system, on the one hand, a small machine armature winding inductance is preferred in order to lower the voltage drop when the machine is loaded; on the other hand, the winding inductance is supposed to be big enough to prevent a high short-circuit current. Therefore, two contradictory conclusions have to be faced on the choice of winding inductance.

However, when adopting the PWM rectifier and its corresponding field-weakening control in a wide-speed-range PMSG system, the voltage regulation when the machine is loaded can be tuned (mainly decreased) by the effect of field-weakening d-axis current id. As a matter of fact, a big inductance can be preferred over a small inductance, considering the voltage regulation and the short-circuit current. In order to design a PMSG suitable for wide-speed-range operation with largely adjustable field and low short-circuit current, a large inductance is needed, which can be achieved by increasing the stator size to put more turns per coil in, while decreasing the rotor size to reduce the size of the magnets.

According to the foregoing analysis, a PMSG has been designed and manufactured for the 1kW 270V DC power system over the speed range of 150~1500r/min (indicated in Table 1), as presented in Fig.6 and Fig.7, respectively. The measured values of the PMSG parameters are listed in Table 2. The field-weakening coefficient is defined and calculated as $K_{fw}=\psi_m/(L_d I_m)\approx 1.32$. It shows a strong field-weakening ability since the value is close to 1, while the smaller value indicates a better field-weakening ability. The capacitance C on the DC-link is about 5000μF, which is relatively big and can lead to a relatively big open-loop time constant of u_{dc}.

Table 1 Specifications of PMSG system

Parameters	Value
Rated DC-link voltage u_{dc}^*/V	270
Base speed n_b/(r/min)	1000
Rated speed n_N/(r/min)	1000
Rated DC power P_{N_dc}/kW	1.0
Efficiency of AC/DC converter η_{conv} /%	95
Rated AC line-line voltage (RMS) U_{N_ac}/V	200
Rated AC power P_{N_ac}/kW	1.05
Rated AC current (RMS/amplitude) I_{N_ac}/A	3.57/5.04
Rated mechanical torque T_N/(N·m)	10.9

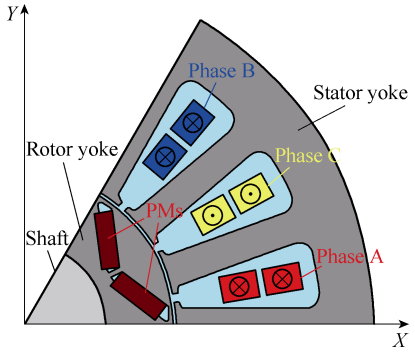

Fig.6 One-pole geometry of PMSG prototype in FEA

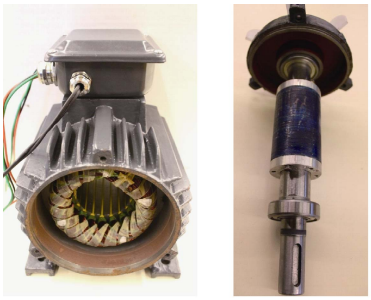

Fig.7 Manufactured PMSG

Table 2 Measured PMSG Parameters

Parameters	Value
Stator resistance per phase R_s/Ω	3.06
Number of pole pairs p	3
d-axis inductance L_d/mH	77
q-axis inductance L_q/mH	153
OC line-line voltage (RMS) at 1000r/min $U_{L\text{-}L}$/V	197

4 Control strategies and comparative study

As a fundamental control strategy, the traditional VC (system configuration in Fig.8(a)) as well as the DTC (see Fig.8(b)) have been analyzed and implemented with the following steps and methods, which are the same as for the proposed DVC (see Fig.8(c)). All of the corresponding simulations and experimental work have been done under the same conditions.

4.1 Small-signal modeling

A PMSG system is modeled according to an existing test bench as described in [24], and shown in Fig.9. It consists of the designed and studied PMSG driven by a speed-controlled prime mover, and the generated power of the PMSG is regulated by a voltage- controlled PWM rectifier, and the generated DC power is supplied to a DC-link, with a capacitor filter and the load.

The output electromagnetic power P_e generated by the PMSG without considering the copper loss (when the stator resistance R_s is negligible compared to the d- and q-axis reactance X_d, X_q at a certain operational speed) is

$$P_e=\frac{3}{2}\left[\frac{E_m U_m}{X_d}\sin\delta+\frac{1}{2}\left(\frac{1}{X_q}-\frac{1}{X_d}\right)U_m^2\sin 2\delta\right] \quad (6)$$

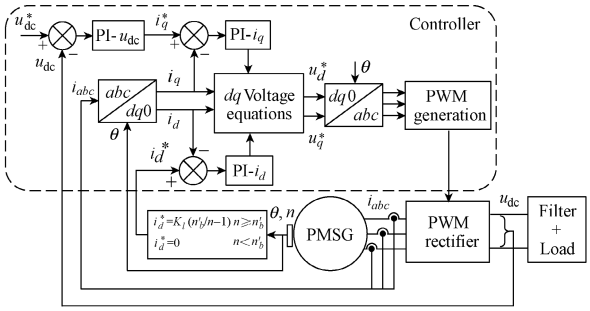

(a) VC

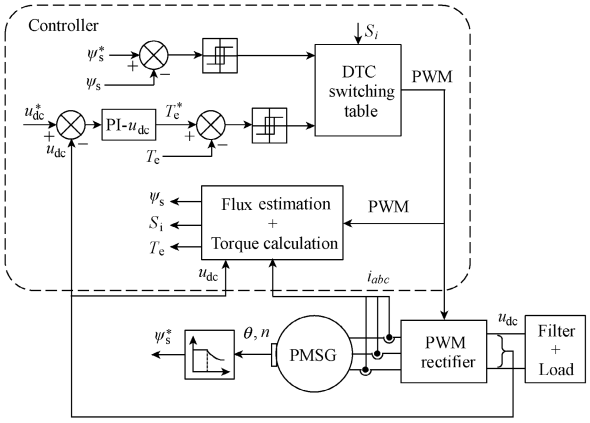

(b) DTC

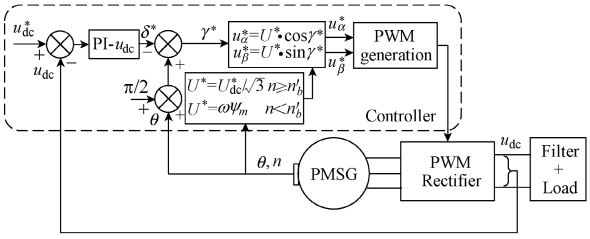

(c) DVC

Fig.8 Various control strategies for PMSG system

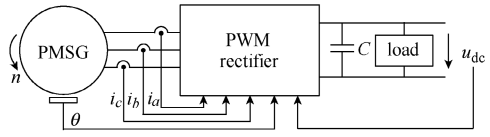

Fig.9 PMSG system configuration

where E_m is the amplitude of the back EMF vector $\boldsymbol{E}$ which is the product of the electrical angular speed ω ($\omega=p\times\Omega$, p is the number of pole pairs and Ω is the machine mechanical angular speed) and the PM-excited flux linkage ψ_m, U_m is the amplitude of the stator voltage vector $\boldsymbol{U}$, and δ is the power angle between $\boldsymbol{E}$ and $\boldsymbol{U}$. Pe can be decided by U_m and δ. The maximum value of U_m is $U_{max}= u^*_{dc}/\mathrm{sqrt}(3)$ according to the features of space-vector PWM (SVPWM) module, where u^*_{dc} is the expected DC-link voltage. Therefore, the modulation index m ($0\leqslant m\leqslant 1$) of the SVPWM module is the ratio of U_m over U_{max}.

The output electromagnetic power is supposed to be consumed on the DC-link without considering the converter losses, hence,

$$P_e = u_d i_d + u_q i_q = u_{dc} C \frac{\mathrm{d}u_{dc}}{\mathrm{d}t} + u_{dc} i_o \tag{7}$$

where C is the capacitance on the DC-link, u_{dc} and i_o are the instantaneous values of the voltage and load current on the DC-link, u_d, i_d and u_q, i_q are the instantaneous d- and q-axis components of armature voltage and current, respectively. The small-signal model of (7) in the frequency domain is obtained without considering the second-order signal perturbations, so as to obtain the open-loop transfer function between $i_o(s)$ and $u_d(s)$:

$$\frac{i_o(s)}{u_d(s)} = \frac{\Delta i_o}{\Delta u_d} = -\frac{3}{2}\left(\frac{\omega L_q I_d - U_q}{\omega L_q u_{dc}}\right) \tag{8}$$

4.2 PI control design

By approximating $U_q \approx \omega L_d I_d + \omega \psi_m$ where the stator resistance R_s and the dynamics of i_q are ignored, there is

$$\frac{i_o(s)}{u_d(s)} = \frac{3}{2}\left(\frac{\psi_m + (L_d - L_q) I_d}{L_q u_{dc}}\right) = G_{u_d - i_o}(s) \tag{9}$$

and u_d is the product of U_m and $\sin\delta$, where $\sin\delta$ tends to δ when δ tends to 0 based on the limitation theory. Therefore, the open-loop transfer function of u_{dc} can be calculated as

$$G_{OL}(s) = K_i \frac{1 + (K_p / K_i)s}{s} \times U_m \times \frac{3}{2}\left(\frac{\psi_m + (L_d - L_q) I_d}{u_{dc} L_q}\right) \times \frac{R_L}{1 + R_L C s} \tag{10}$$

with the pole-zero cancellation ($K_p/K_i=R_LC$), (10) becomes

$$G_{OL}(s) = \frac{3(\psi_m + (L_d - L_q) I_d) U_m R_L K_i}{2 u_{dc} L_q s} \tag{11}$$

Taking $U=m\cdot u_{dc}/\mathrm{sqrt}(3)$, the closed-loop transfer function of u_{dc} becomes

$$G_{CL}(s) = \frac{G_{OL}(s)}{1 + G_{OL}(s)} = \frac{1}{1 + \dfrac{2L_q}{\sqrt{3} m (\psi_m + (L_d - L_q) I_d) R_L K_i} s} \tag{12}$$

where the closed-loop time constant τ_{CL} is

$$\tau_{CL} = \frac{1}{2\pi f_{CL}} = \frac{2L_q}{\sqrt{3} m (\psi_m + (L_d - L_q) I_d) R_L K_i} \tag{13}$$

By well choosing a cut-off frequency f_{CL}, where $\tau_{CL}=1/(2\pi f_{CL})$, the proportional coefficient K_p and the integral coefficients K_i can be calculated as:

$$K_p = \frac{4\pi f_{CL} L_q C}{\sqrt{3} m (\psi_m + (L_d - L_q) I_d)} \tag{14}$$

$$K_i = \frac{4\pi f_{CL} L_q}{\sqrt{3} m (\psi_m + (L_d - L_q) I_d) R_L} \tag{15}$$

and the corresponding control scheme of DVC[23] can be drawn as in Fig.10.

4.3 Active damping

The system is supposed to have the ability to withstand a sudden load change, by applying the same theory of active damping which is commonly used for the motor speed control. In this PMSG-based DC power system, the active damping can be added to the control by means of a fictitious resistor $R_{L,\mathrm{act}}$ connected in parallel with the load and making a new control scheme with a decreased total resistance $R_{L,\mathrm{tot}}$ (i.e., $R_{L,\mathrm{tot}}=R_L\cdot R_{L,\mathrm{act}}/(R_L+R_{L,\mathrm{act}})$ on the DC-link (see Fig.11).

The proportional and integral coefficients K_p' and K_i' considering the active damping can be calculated by applying the same pole-zero cancellation method as previously.

$$K_\mathrm{p}'=\frac{2\pi f_{CL}\left(\psi_\mathrm{m}+\left(L_d-L_q\right)i_d^*\right)u_\mathrm{dc}C}{\Omega\psi_\mathrm{m}} \tag{16}$$

$$K_i'=\frac{2\pi f_{CL}\left(\psi_\mathrm{m}+\left(L_d-L_q\right)i_d^*\right)u_\mathrm{dc}}{\Omega\psi_\mathrm{m}R_{L,\mathrm{tot}}} \tag{17}$$

$K_\mathrm{p}'=K_\mathrm{p}$ while K_i' is bigger than K_i as in (11) and (12). The control scheme considering active damping is shown in Fig.12.

The active damping gain K_{ad} is derived as

$$K_{ad}=\frac{\left(\psi_\mathrm{m}+\left(L_d-L_q\right)i_d^*\right)u_\mathrm{dc}}{\Omega\psi_\mathrm{m}R_{L,\mathrm{act}}} \tag{18}$$

According to the gauge of the armature windings, there exists the allowed maximum current I_m in order to limit the temperature rise and further machine damage. Here, I_m can be set to the amplitude of the rated armature current Ir. Moreover, the stator voltage U_m is restricted by the DC-link voltage u_dc and the modulation index m. The sets of d- and q-axis armature currents (I_d, I_q) satisfying the curve of the electromagnetic power should be within the current and voltage limitations.

The base speed n_b at no load is defined as:

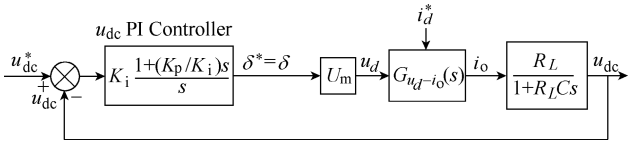

Fig.10 Control scheme of DVC

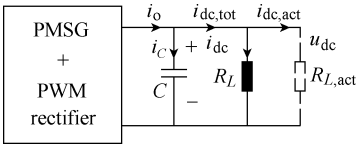

Fig.11 DC-Link model with active damping

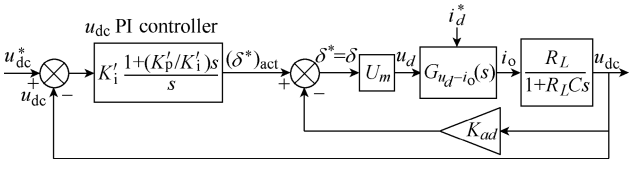

Fig.12 Control scheme of DVC with active damping

$$E_\mathrm{m}=p\frac{2\pi n_b}{60}\psi_\mathrm{m}=U_{\max}=\frac{u_\mathrm{dc}^*}{\sqrt{3}} \tag{19}$$

and U_m is equal to the product of m and $U_{\max}$. The operational speed is $n_b\leqslant n\leqslant n_{\max}$($n_{\max}$ is the maximum operational speed), m=1; whereas the operational speed is $n<n_b$, m can be calculated according to the speed.

4.4 Simulation analysis of direct voltage control

The simulation model is built in Matlab/Simulink. The reference DC-link voltage u_dc^* is fixed at 270V. Different operational speeds within the wide speed range, i.e., 150, 500, 1000, 1500r/min, are tested, with a load variation at 1s in each case. The simulation results of u_dc without and with active damping are compared in Fig.13.

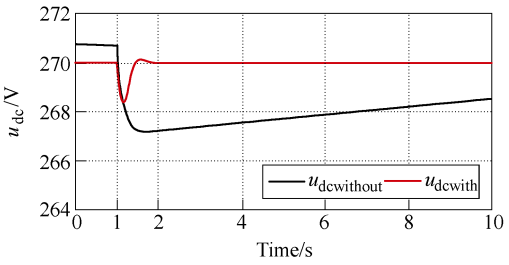

(a) 150r/min

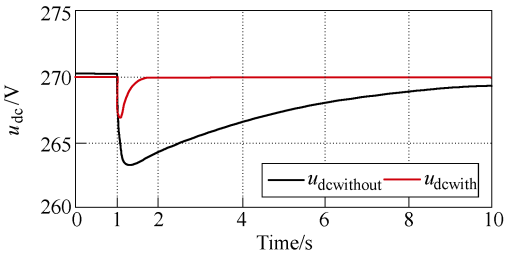

(b) 500r/min

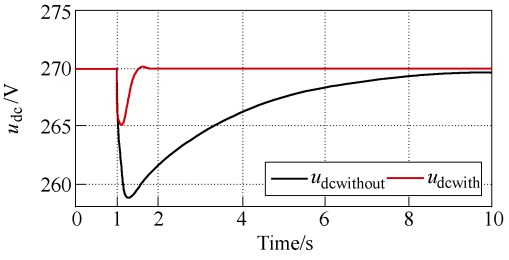

(c) 1000r/min

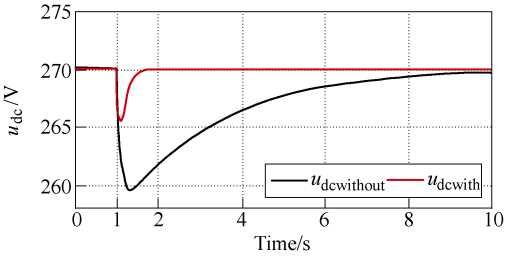

(d) 1500r/min

Fig.13 Simulation results of u_dc under DVC with sudden load variation

As the stator resistance R_s (R_s=3.06Ω) cannot be neglected at the lowest operational speed (150r/min), where the d- and q-axis reactances X_d and X_q ($X_d \approx 3.63\Omega$, $X_q \approx 7.21\Omega$) are not big enough, the DVC has a fatal problem of inaccuracy under the approximation of R_s being ignored. From the simulation results at each tested speed, active damping can effectively decrease the closed-loop time constant and speed up the DC-link voltage response.

4.5 Experimental results of direct voltage control

Fig.14 shows the test bench, where the studied PMSG is driven by a speed-controlled PMSM. The test bench encounters a noise from time to time, which may affect the system performance. The PMSG serves as a load of the prime mover, therefore, the variation of the working condition of the PMSG will have an impact on the speed of the prime mover. In other words, when the load is suddenly applied on the DC-link, the speed of the PMSM and PMSG will be disturbed. Due to this imperfection of the speed control of the PMSM, the performance of the PMSG will be affected, with more severe ripples in the DC-link voltage u_{dc} and the load angle δ. The experimental results corresponding to Fig.13 are shown in Fig.15, respectively. In general, the experimental results agree with the simulation results.

4.6 Comparative study in experiments

In the experiments, the parameters of each PI controller are adaptive, varying with the DC-link voltage reference u_{dc}^*, the load resistance RL, the mechanical angular speed Ω under VC, DTC, and the modulation index m of SVPWM module under DVC. Note, m can always be 1 during flux-weakening operation.

Since the prime mover is not perfectly speed-controlled, there is speed variation especially when the working conditions of the PMSG are varying, e.g., the DC-link voltage reference or the equivalent load resistance is changed.

The experimental results at both steady-state and transient-state of VC, DTC and DVC are also compared in Table 3 (the DC-link voltage ripple (peak-to-peak value)), Table 4 (the armature current THD), Table 5 (the DC-link voltage drop at load increase), and Table 6 (the DC-link voltage recovery time). At low speeds, the DTC has the most severe DC-link voltage ripple, while in the field-weakening region, the voltage ripple in the DVC is the most obvious. Small armature current THD can be noticed in the VC, while the DTC has the severest current THD due to the absence of current loops. A flux observer is needed in the DTC,

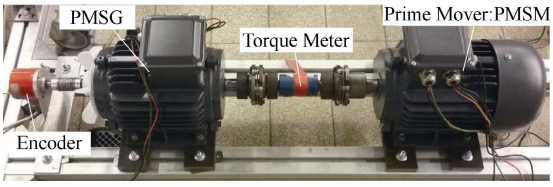

Fig.14 Test bench description

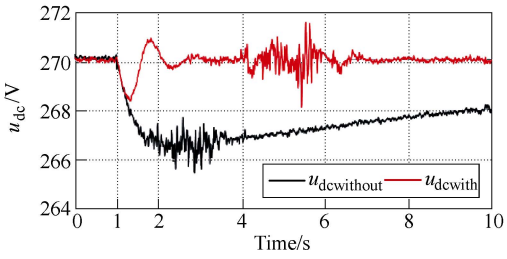

(a) 150r/min

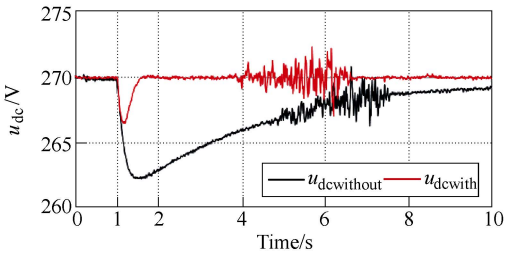

(b) 500r/min

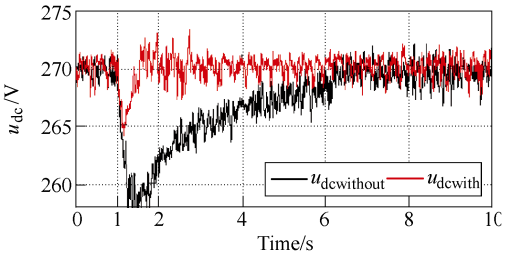

(c) 1000r/min

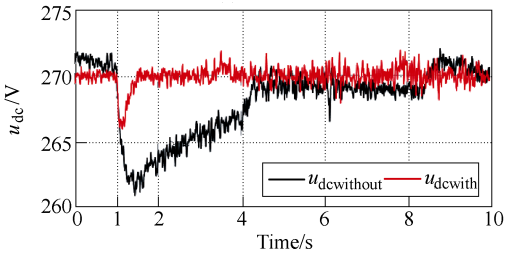

(d) 1500r/min

Fig.15 Experimental results of u_{dc} under DVC with sudden load variation

Table 3 DC-link voltage ripple (peak-to-peak value)

Tested speed/(r/min)	VC/V	DTC/V	DVC/V
150	0.2	1.6	0.3
500	0.4	0.8	0.2
1000	0.6	1.2	3.0
1500	1.0	2.0	2.0

Table 4 Armature current THD

Tested speed/(r/min)	VC (%)	DTC (%)	DVC (%)
150	2.95	39.34	8.26
500	6.08	56.42	7.59
1000	14.34	34.90	24.34
1500	9.30	17.67	10.30

Table 5 DC-link voltage drop at load increase

Tested speed/(r/min)	VC/V	DTC/V	DVC/V
150	1.0	0.8	1.6
500	4.0	3.5	3.4
1000	4.3	6.0	5.0
1500	3.5	3.2	3.5

Table 6 DC-link voltage recovery time

Tested speed/(r/min)	VC/s	DTC/s	DVC/s
150	3.0	1.2	2.6
500	2.2	2.2	1.6
1000	2.2	2.1	1.6
1500	1.4	1.5	1.5

which makes it a complex system. The DVC can enhance the system's fault tolerance against the current sensor faults, since no current loop is included and the control scheme is greatly simplified. The results of voltage excursion (voltage drop at load increase) and the recovery time show little difference but all the studied control strategies are effective in the DC-link voltage regulation.

5 Conclusion

DC power systems are becoming more and more popular in various industrial applications. PMSGs are superior candidates in these applications, the generated electrical power of which can be regulated by an active rectifier in order to obtain a constant DC-link voltage. DVC has been proposed and studied in detail, with the system analysis and calculation of the adaptive PI controller for the DC-link voltage. The simulation model has been built in Matlab/Simulink, according to an existing test bench including one PM machine being the prime mover and another PM machine being the generator. Both VC and DTC have also been employed to compare with the DVC both in simulation and experiments. All of the aforementioned systems have been proven to be effective, which can output a stable DC-link voltage over a wide operational speed range (150~1500r/min in this case), supplied by a PMSG with strong field-weakening ability and a PWM rectifier controlled by different strategies, i.e., the VC, DTC and DVC.

There are current control loops in the VC, small current THD can therefore be noticed. There are no current loops in the DTC, instead, the flux observer is needed, hence, the control scheme is complex, and the voltage and torque ripples are obvious. The DVC enhances the system's fault tolerance against current sensor faults, since no current loop is included, and the control system structure is greatly simplified.

References

[1] G. C. Lazaroiu, D. Zaninelli, M. O. Popescu, and M. Roscia, "Grid connected and stand alone DC power system prototype", *IEEE Int. Conf. Harmonics and Quality of Power*, pp. 529-534. 2012.

[2] J. Chen, J. W. Chen, C. Y. Gong, and X. Deng, "Energy management and power control for a stand-alone wind energy conversion system," *IEEE Industrial Electronics Society Conf.*, pp. 989-994, 2012.

[3] X. B. Yuan, and Y. D. Li, "Control of variable pitch and variable speed direct-drive wind turbines in weak grid systems with active power balance," *IET Renewable Power Generation*, vol. 8, no. 2, pp. 119-131, Mar. 2014.

[4] H. Zhang, C. Saudemont, B. Robyns, N. Huttin, and R. Meuret, "Stability analysis on the DC power distribution system of more electric aircraft," in *Proc. 2008 IEEE Power Electronics and Motion Control Conf.*, pp. 1523-1528.

[5] F. Gao, X. C. Zheng, S. Bozhko, C. I. Hill, and G. Asher, "Modal analysis of a PMSG-based DC electrical power system in the more electric aircraft using eigenvalues sensitivity," *IEEE Trans. Transportation Electrification*, vol. 1, no. 1, pp. 65-76, Jun. 2015.

[6] K. W. Hu, and C. M. Liaw, "Incorporated operation control of DC microgrid and electric vehicle," *IEEE Trans. Industrial Electronics*, in press.

[7] E. Mese, Y. Yasa, H. Akca, M. G. Aydeniz, M. Ayaz, and M. Tezcan, "Investigating converter options for automotive grade permanent magnet synchronous generators," *IEEE Electric Power and Energy Conversion Systems Conf.*, pp. 1-5, 2013.

[8] D. Seyoum, M. F. Rahman, and C. Grantham, "Terminal voltage control of a wind turbine driven isolated induction generator using stator oriented field control," *IEEE 8th Annual Conference on Applied Power Electronics Conference and Exposition*, Miami Beach, FL, USA, 2003, vol.2, pp.846-852.

[9] M. M. Amin, and O. A. Mohammed, "DC-bus voltage control of three-phase PWM converters connected to wind powered induction generator," *IEEE Power and Energy Society General Meeting*, pp. 1-7, 2010.

[10] M. M. N. Amin, and O. A. Mohammed, "DC-bus voltage control technique for parallel-integrated permanent magnet wind generation systems," *IEEE Trans. Energy Conversion*, vol. 26, no. 4, pp. 1140-1150, Dec. 2011.

[11] M. M. N. Amin, B. Mirafzal, and O. Mohammed, "A DC-bus voltage regulation for parallel wind-based synchronous generators," *Annual Conference of IEEE Industrial Electronics Society*, Glendale, AZ, pp. 3161-3166, 7-10 Nov. 2010.

[12] M. M. Amin, and O. A. Mohammed, "Design and implementation of DC-bus system module for parallel integrated sustainable energy conversion systems," *IEEE Power and Energy Society General Meeting*, San Diego, CA, pp. 1-8, 24-29 July 2011.

[13] Z. Zhang, Y. Zhao, W. Qiao, and L. Y. Qu, "A space-vector-modulated sensorless direct-torque control for direct-drive PMSG wind turbines," *IEEE Trans. Industry Applications*, vol. 50, no. 4, pp. 2331-2341, Jul./Aug. 2014.

[14] R. Bojoi, M. G. Neacsu, and A. Tenconi, "Analysis and survey of multi-phase power electronic converter topologies for the more electric aircraft applications,"*International Symposium on Power Electronics, Electrical Drives, Automation and Motion*, Sorrento, Italy, pp. 440-445, 20-22 Jun. 2012.

[15] Y. Deng, S. Y. Foo, and I. Bhattacharya, "Regenerative electric power for more electric aircraft," *IEEE Southeast CON*, Lexington, KY, USA, pp. 1-5, 13-16 Mar. 2014.

[16] Y. Hu, W. Huang, and Y. Li, "A novel instantaneous torque control scheme for induction generator systems," *IEEE Transactions on Energy Conversion*, vol.25, no.3, pp. 795-803, Sep. 2010.

[17] M. Sinnett, "787 no-bleed system: saving fuel and enhancing operational efficiencies," *Boeing Aero*, qtr_04, 2007, pp. 6-11.

[18] Y. Hu, W. Huang, and Y. Li, "A novel instantaneous torque control scheme for induction generator systems," *IEEE Transactions on Energy Conversion*, vol.25, no.3, pp. 795-803, Sep. 2010.

[19] R. T. Naayagi, "A review of more electric aircraft technology," *IEEE International Conference on Energy Efficient Technologies for Sustainability*, Nagercoil, India, pp. 750-753, 10-12 Apr. 2013.

[20] J. A. Weimer, "Electrical power technology for the more electric aircraft," *AIAA/IEEE Digital Avionics Systems Conference*, Fort Worth, TX, USA, pp. 445-450, 25-28 Oct. 1993.

[21] J. A. Weimer, "The role of electric machines and drives in the more electric aircraft," *IEEE International Electric Machines and Drives Conference*, Madison, Wisconsin, USA, vol. 1, pp. 11-15, 1-4 Jun. 2003.

[22] L. J. He, Y. D. Li, and R. G. Harley, "Adaptive multi-mode power control of a direct-drive PM wind generation system in a microgrid," *IEEE Journal of Emerging and Selected Topics in Power Electronics*, vol. 1, no. 4, pp. 217-225, Dec. 2013.

[23] D. M. Miao, Y. Mollet, J. Gyselinck, and J. X. Shen, "Direct voltage field-oriented control for permanent-magnet synchronous generator systems with an active rectifier," unpublished, will be presented at the *IEEE Int. Energy Conf*., Leuven, Belgium, 2016.

[24] D. M. Miao, Y. Mollet, J. Gyselinck, and J. X. Shen, "DC voltage control of a wide-speed-range permanent-magnet synchronous generator system for more electric aircraft applications," *The 13th IEEE Vehicle Power and Propulsion Conference*, Hangzhou, China, 17-20 Oct. 2016.

Dongmin Miao was born in Hangzhou, China, in 1988. She received the B.Eng. degree from Zhejiang University, Hangzhou, China, in 2007, and the double Ph. D. degrees from Zhejiang University and Université Libre de Bruxelles, Brussels, Belgium, in 2016, all in electrical engineering. Her main research interests include the PM machine design and different motor/generator control strategies.

Yves A. B. MOLLET received the master in electromechanical industrial engineering from the Haute Ecole Léonard de Vinci (ECAM), Brussels, Belgium, in 2010.

He is currently a Ph. D. student at the Université Libre de Bruxelles, Brussels, Belgium and performs at present a secondment at Siemens Industry Software, Leuven, Belgium. His main research topics include fault detection in wind power systems (using DFIGs and PMSMs) and electrical vehicles.

Johan J. C. GYSELINCK received the M.S. degree in electrical and mechanical engineering and the Ph.D. degree in applied sciences from Ghent University, Gent, Belgium, in 1991 and 2000, respectively. From 2000 to 2004, he was a Postdoctoral Researcher at the Applied and Computational Electromagnetics research unit of the University of Liège, Liège, Belgium.

He is currently an Associate Professor with the Université Libre de Bruxelles, Brussels, Belgium, and his research mainly concerns the numerical computation of magnetic fields, the simulation and control of electrical machines and drives, and renewable energy systems.

Jianxin Shen was born in Huzhou, China, in 1969. He received the B.Eng. and M.Sc. degrees from Xi'an Jiaotong University, Xi'an, China, in 1991 and 1994, respectively, and the Ph. D. degree from Zhejiang University, Hangzhou, China, in 1997, all in electrical engineering.

He was with Nanyang Technological University, Singapore(1997-1999), the University of Sheffield, Sheffield, U.K. (1999-2002), and IMRA Europe SAS, U.K. Research Centre, Brighton, U.K. (2002-2004). Since 2004, he has been a Professor of Electrical Engineering with Zhejiang University.

Prof. Shen has authored more than 220 technical papers, and holds 39 patents. He received a Prize Paper Award from the IEEE Industry Applications Society and best paper awards from five international conferences, and was a Keynote Speaker for three international conferences. He was the General Chair of two IEEE (co-)sponsored international conferences. His main research interests include topologies, control and applications of permanent magnet machines and drives, and renewable energies.

More information of Prof. Shen can be seen at http://mypage.zju.edu.cn/en/jxs. He is the corresponding author and can be contacted at J_X_Shen@zju.edu.cn.